Biosensors and Bioelectronics 38 (2012) 245–251

Contents lists available at SciVerse ScienceDirect

Biosensors and Bioelectronics

journal homepage: www.elsevier.com/locate/bios

Voltammetric investigation of DNA damage induced by nitrofurazone and short-lived nitro-radicals with the use of an electrochemical DNA biosensor

Yongnian Ni [a,b,*], Pingping Wang [b], Serge Kokot [c]

[a] State Key Laboratory of Food Science and Technology, Nanchang University, Nanchang 330047, China
[b] Department of Chemistry, Nanchang University, Nanchang 330031, China
[c] School of Chemistry, Physics and Mechanical Engineering, Science and Engineering Faculty, Queensland University of Technology, Brisbane 4001, Australia

ARTICLE INFO

Article history:
Received 20 March 2012
Received in revised form
17 May 2012
Accepted 28 May 2012
Available online 6 June 2012

Keywords:
dsDNA/GCE biosensor
Nitrofurazone
DNA-damage
Nitro-radicals
Atomic force microcopy
$Co(phen)_3^{2+}$ probe

ABSTRACT

Electrochemical behavior of nitrofurazone (NFZ) was investigated with the use of cyclic voltammetry (CV) and differential pulse voltammetry (DPV) methods. The pH-dependence of NFZ was studied at a glassy carbon electrode (GCE) in ethanol/Britton–Robinson buffer (30:70), and short-lived nitro-radicals were generated by the reduction of NFZ at high pHs (>7.0). In the presence of DNA, the DPV peak current of NFZ decreased and the peak potential shifted negatively, which indicated that there was an electrostatic interaction between NFZ and DNA. An electrochemical dsDNA/GCE biosensor was prepared to study the DNA damage produced in the presence NFZ; this process was followed with the use of the $Co(phen)_3^{2+}$ electroactive probe. Also, the oxidation peaks of guanosine (750 mV) and adenosine (980 mV) indicated that DNA damage was related directly to the nitro-radicals. Experiments demonstrated that DNA damage occurred via two different steps while NFZ was metabolized and nitro-radicals were produced. Novel work with AFM on the NFZ/DNA interaction supported the suggestion that *in vivo*, the nitro-radicals were more cytotoxic than the NFZ molecules. A linear DPV calibration plot was obtained for NFZ analysis at a modified dsDNA/GCE (concentration range: 2.50×10^{-6}–3.75×10^{-5} mol L^{-1}; limit of detection: 8.0×10^{-7} mol L^{-1}), and NFZ was determined successfully in pharmaceutical samples.

1. Introduction

In general, complementary and supplementary electrochemical techniques are often useful to study small molecule/biopolymer (proteins or DNA) interactions in different aqueous media. Such reactions commonly involve redox processes, which often damage the host bio-molecule. This study is focused on the interaction of the nitrofurazone (NFZ) and its potential to damage DNA; cyclic voltammetry (CV) and differential pulse voltammetry (DPV) were the analytical techniques of choice. NFZ is a synthetic nitrofuran derivative, and on the one hand, it is an effective fungicide, amoebicide and skin sensitizer used against various allergies and infections animals and humans (de Bengoa Vallejo et al., 2011; Trossini et al., 2010; Escobosa et al., 2009) as well as in aquaculture (Tittlemier et al., 2007), but on the other hand, in recent years, this antimicrobial drug has been linked with carcinogenic effects, particularly, in large doses (Ito et al., 2005; Takahashi et al., 2000; Takegawa et al., 2000; Bartel et al., 2009). At present, the International Agency for Research on Cancer (IARC) categorizes NFZ as a Group 3 drug i.e. it is not deemed to be carcinogenic to humans (International Agents for Research on Cancer (IARC), 2011). Consequently, studies of the interaction of NFZ with DNA and the mechanism involved are of interest and importance.

In this context, Hiraku et al. (2004) reported that NFZ could be metabolized by cytochrome P450 to produce short-lived nitro-radicals; their electron spin resonance spectroscopy investigations showed that radicals were generated from NFZ, and found that NFZ metabolites (nitro-radicals) were involved in tumor initiation by facilitating oxidation of DNA; also, NFZ itself participated in tumor promotion and progression through enhancement of cell proliferation.

Ona et al. (2009) reported that NFZ was reduced by cellular nitroreductases to form N^2-deoxyguanine adducts that were associated with mutagenesis and toxicity; they also found that nucleotide excision repair was a primary mechanism for processing damage induced by NFZ. Zhou et al. (2011) found that ciliates, treated with NFZ, produced damaged DNA. These conclusions were made on the basis of results of a random amplified polymorphic DNA (RAPD) assay. Thus, these studies indicated that NFZ itself and its metabolites could be cytotoxic in cellular systems. Apart from the RAPD method, the PCR bioanalysis (Ito et al., 2005) and the high

* Corresponding author at: Department of Chemistry, Nanchang University, Nanchang 330031, China. Tel./fax: +86 791 83969500.
E-mail addresses: ynni@ncu.edu.cn (Y. Ni), s.kokot@qut.edu.au (S. Kokot).

0956-5663/$ - see front matter © 2012 Elsevier B.V. All rights reserved.
http://dx.doi.org/10.1016/j.bios.2012.05.034

performance liquid chromatography (HPLC; electrochemical detector; Hiraku et al., 2004) have been used with similar indicative results. However, in general, these techniques are time-consuming, and involve costly equipment and maintenance. Electrochemical methods of analysis, especially those involving electrochemical biosensors, offer simple, relatively cheap equipment with rapid detection as alternative applications (Zhang et al., 2010b; Xu et al., 2011; Xiong et al., 2011). For dsDNA, the two strands of nucleotides are twisted into a double helix, held together by hydrogen bonds between the adenine(A)–thymine(T) and guanine(G)–cytosine(C) bases of each strand. Thus, it is very difficult to detect the electrochemical signals of these four bases. However, when DNA is damaged by free-radicals, the double helix of the DNA will be broken and this will facilitate the oxidation of the bases (especially guanine) or generate DNA adducts. Such drastic changes to the DNA structure would affect the subsequent replication and transcription of DNA, and this may lead to cancer. However, DNA damage is difficult to detect directly by applying electrochemical analysis particularly with guanosine and adenosine because the bases are shielded by the dsDNA, which interferes with the electron transfer to the electrode's surface. Thus, an indirect method with the use of redox electroactive probes (Zhang et al., 2010a; Liao et al., 2010), has been used in this work—specifically the $Co(phen)_3^{2+}$ complex.

DNA biosensors have been previously used to study DNA damage induced by short-lived nitro-radicals (Abreu et al., 2002; Vyskočil et al., 2010), and the reduction of nitro-aromatic compounds to generate nitro-radicals was achieved as follows: 1. by successive CV cathodic scanning, and 2. reduction at a fixed potential. The first method showed that if the nitro-aromatic reduction was facilitated by successive cathodic cycling, the DNA damage was more severe when compared to that produced by reduction at a fixed potential. It appeared that the damage increased when short-lived nitro-radicals were freshly generated during sequential reduction of the NFZ during the CV cycling. However, interestingly, in these investigations, the production of nitro-radicals was assumed and no direct evidence of their existence was presented. In contrast, voltammetric analysis showed that ethyl-*m*-nitrobenzoate disproportionated in water/DMF, and a nitro-radical formed (Carbajo et al., 2000). Similar studies of the NZF molecule in protic, mixed and aprotic media indicated that reduction of the nitro-radical anion was present in all three media (Bollo et al., 2005). In addition, kinetics research of the related reactions further supported the formation of the nitro-radicals (Fotouhi and Faramarzl, 2004). These studies provided the basis to further explore the potential role of the nitro-radical anion, derived from the NFZ, in induction of carcinogenesis.

Recently, the investigation of the toxicity of NFZ has focused on its presence as a food residue, and many techniques have been used for its analysis e.g. HPLC (Lin and Jeng, 2001), cathodic stripping voltammetric (Khodari et al., 1999) and others (Wang and Zhang, 2006; Thongsrisomboon et al., 2010; Tubino et al., 2009). Chen et al. (2010) synthesized a new fluorescence sensor to analyze NFZ.

Thus, the aims of this work were: 1. to investigate the chemistry of the nitro-radicals generated by the reduction of the NFZ in protic media with the use of electrochemical techniques; 2. to use a DNA biosensor to investigate the interaction of DNA with NFZ in the same media, and to establish if the DNA was damaged by the nitro-radical and/or the NFZ molecule itself and 3. to develop a method for quantitative analysis of NFZ by the DNA biosensor.

2. Experimental

2.1. Chemicals

Double-stranded calf thymus DNA (type I, No. D1501; Sigma-Aldrich Co., Shanghai) and nitrofurazone (NFZ; Sigma-Aldrich Co., Shanghai) were used as received. DNA solution (1.0 mg mL^{-1}) was prepared by dissolving 50.0 mg of the solid in 50 mL 50 mmol L^{-1} sodium chloride solution. NFZ stock solution (5×10^{-3} mol L^{-1}) was prepared by dissolving 0.1 g crystals in 100 mL dimethylformamide (DMF). $[Co(phen)_3](ClO_4)_2 \cdot 2H_2O$ solution (5.0 mmol L^{-1}) was prepared by dissolving the crystals (0.4670 g) in 100 mL 10 mmol L^{-1} phosphate buffer (pH=7.00). Ethanol/Britton–Robinson buffer (30:70, v/v), a protic medium, was the electrolyte. Sample solutions were purged with pure nitrogen for 5 min prior to any measurements. All chemicals were Analytical Grade reageants and double-distilled water was used throughout.

2.2. Instrumentation

CV and DPV experiments were performed with the use of a CHI 660 A electrochemical workstation (CH Instruments, Shanghai, China). A conventional three-electrode system was used for the measurements, and it was equipped with a glassy carbon electrode (GCE, 3 mm diameter) or a modified dsDNA/GCE as the working electrode, a platinum auxiliary and an Ag/AgCl reference electrodes. Atomic force microscope (AFM) was the AJ-III model (Shanghai Aijian Nanotechnology) in the tapping mode. Standard silicon cantilevers (spring constant, 0.6–6 N/m) were used at their typical resonance frequencies e.g. 60–150 kHZ. Mica sheets were from the General Research Institute (Shanghai). Buffer pH was monitored with an Orion SA720 meter (US). All experiments were carried out at 25 ± 0.5 °C.

2.3. Preparation of the dsDNA/GCE

The GCE was polished sequentially with 1.0, 0.3 and 0.05 μm alumina slurry on a polishing felt, and then, the electrode was sonicated in 0.5 mol L^{-1} dilute nitric acid, ethanol and deionized water, sequentially, for 5 min at a time. After gentle mechanical cleaning, the GCE was further cleaned by repeated potential scanning between −1.0 and 1.0 V in 10 mL 0.25 mol L^{-1} sulfuric acid until a reproducible cyclic voltammogram was observed. This procedure activated the electrode surface so as to assist the immobilization of the dsDNA (Pang et al., 1996). The electrode surface was then washed with double-distilled water and left to dry. Subsequently, 30.0 μL 1.0 mg mL^{-1} dsDNA stock solution was deposited on the surface of the GCE and dried for 6 h in air at room temperature. The obtained dsDNA/GCE was washed with deionized water and immersed in a protic medium (pH=9.10) for 2 min to remove any loosely adsorbed DNA. The prepared dsDNA/GCE electrode was then submitted to CV analysis in the presence of 5.0 mmol L^{-1} $[Fe(CN)_6]^{3-/4-}$ (dissolved in 0.1 mol L^{-1} KCl) as an electroactive probe; the potential was scanned from −0.1 to 0.6 V with a scan rate of 100 mV s^{-1}.

2.4. Immobilization of dsDNA or NFZ–dsDNA on the mica sheet

Mica sheets were freshly cleaved with adhesive tape prior to each experiment, then an AFM image was obtained and sample cleanliness was checked. A thick dsDNA or NFZ–dsDNA film was prepared by covering the mica sheets with 30 μL 1.0 mg mL^{-1} DNA solution (containing 5×10^{-3} mol L^{-1} Mg^{2+}) or a mixed solution (30 μL 1.0 mg mL^{-1} DNA, 5×10^{-3} mol L^{-1} Mg^{2+} and 5×10^{-3} mol L^{-1} NFZ); these films were allowed to stand in a sterile environment to dry overnight before further processing. The thin dsDNA and NFZ–dsDNA films were also prepared by covering the mica sheet with the above solution diluted 100 times.

2.5. Investigation of the electrochemical mechanism: experimental procedures

Experiment 1. pH-dependent behavior of nitrofurazone

400 μL 5.0 mmol L^{-1} nitrofurazone together with 7.0 mL Britton–Robinson buffer (pH 1.98–10.02) and 3.0 mL ethanol were transferred into a 10 mL electrolysis cell, i.e. the concentration of NFZ was 2×10^{-4} mol L^{-1}, and CV was performed over the potential range of −1.4 to 0 V with a scanning rate of 100 mV s^{-1}.

Experiment 2. Interaction between NFZ and dsDNA

NFZ (400 μL of 5.0 mmol L^{-1}) was mixed with a pH 9.10 protic solution (7.0 mL Britton–Robinson buffer mixed with 3.0 mL ethanol) to obtain an NFZ concentration of 2×10^{-4} mol L^{-1}, and DPV was carried out to investigate the interaction between NFZ and dsDNA in this medium. DNA was then added at intervals of 0.005 mg mL^{-1} to produce sequentially, solutions in the concentration range 0–0.020 mg mL^{-1}. At each addition, the potential was scanned from 0 to −0.9 V with a scanning rate of 20 mV s^{-1}, pulse width 60 ms and pulse amplitude 50 mV; thus, five voltammograms were obtained.

Experiment 3. Indirect investigations of the DNA/NFZ interaction for possible DNA damage

A dsDNA/GCE electrode was immersed into a 10 mL 50.0 μM $Co(phen)_3^{2+}$ solution (pH 7.00) for 10 min. Then, the treated dsDNA/GCE electrode was submitted to DPV analysis over a potential range of −0.4 to 0.4 V with a scan rate of 20 mV s^{-1}, pulse width of 60 ms and pulse amplitude of 50 mV. The electrode was washed with double-distilled water and treated for 10 min in 5.0×10^{-3} mol L^{-1} NFZ solution. This treated electrode was then submitted to DPV analysis as described above.

Experiment 4. Direct investigations of the DNA/NFZ interaction for possible DNA damage induced by short-lived nitro-radicals

A DPV analysis involving the dsDNA/GCE was carried out in a blank solution of 10 mL protic medium (pH 9.10) over the potential range of 0 to +1.5 V with a scan rate of 20 mV s^{-1}, pulse width of 60 ms and pulse amplitude of 50 mV. 400 μL 5.0×10^{-3} mol L^{-1} NFZ solution was then added to the solution (NFZ$=2.0 \times 10^{-4}$ mol L^{-1}), and the DPV method was then applied under the same conditions to detect the oxidation of the DNA purine bases in this solution. Finally, consecutive cathodic CV scans were collected at the prepared dsDNA/GCE in a 2.0×10^{-4} mol NFZ solution from 0 to −0.9 V with a scan rate of 100 mV s^{-1} (total: 10 scans); following this experiment, the solution was analyzed with the use of the DPV method under the previously applied conditions as noted above.

2.6. Quantitative analysis of NFZ and its application to a pharmaceutical sample

NFZ solutions with different concentrations were prepared (10 mL pH=9.10 protic medium). Using the DNA biosensor, DPV was performed from 0 to −0.9 V (pulse amplitude of 0.05 V, pulse width of 0.06 and rest time 2 s) and a calibration model was established.

Nasal drops (100 μL) without pretreatment were added to 10 mL pH 9.10 protic medium. DPV was carried out to determine NFZ in this real sample under the same conditions. Then, these solutions were spiked with a series of NFZ standard solutions; these samples were analyzed by DPV to verify the method.

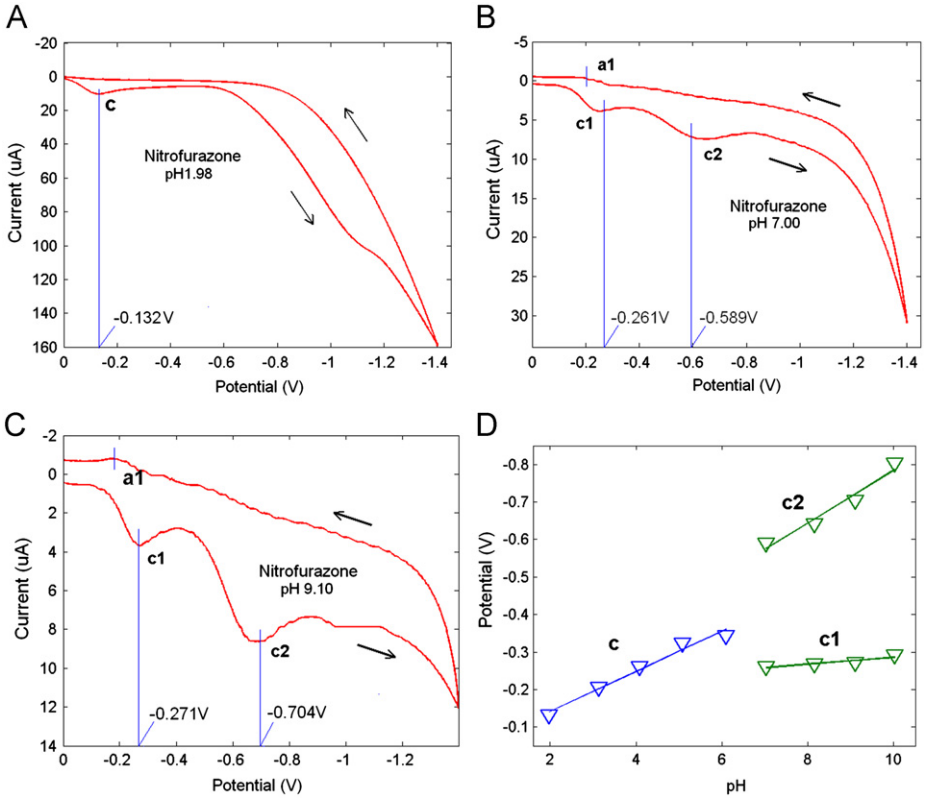

Fig. 1. Cyclic voltammograms of NFZ (2.0×10^{-4} mol L^{-1}) in protic medium (ethanol/Britton–Robinson buffer (30:70)) at different pH: (A) 1.98; (B) 7.00; (C) 9.10, and (D) plots of peak potential versus pH.

3. Results and discussion

3.1. Electrochemical behavior of NFZ

3.1.1. Influence of pH

Behavior of NFZ in the protic media of different pH (Experiment 1, Section 2.4.) indicated (Fig. 1A) that a single cathodic reduction peak (c) of NFZ was obtained at −0.132 V in pH 1.98 medium. This corresponds to a four electron/four proton reaction, forming hydroxylamine (Tocher, 1997)

$$ArNO_2 + 4e^- + 4H^+ \rightarrow ArNHOH + H_2O \quad (1)$$

At pH 7, the reduction mechanism of NFZ changed (Fig. 1B) and two new cathodic peaks, c1 and c2 were observed. These were more pronounced at pH 9.10 (Fig. 1C). It has been suggested that NFZ may be reduced via two different routes depending on the media conditions (da S. Julião et al., 2006). The first step is the one-electron reduction to form the nitro-radical anions

$$ArNO_2 + e^- = ArNO_2^- \quad (2)$$

then, under anaerobic conditions, these radical anions may be further reduced to a hydroxylamine derivative

$$ArNO_2^- + 3e^- + 4H^+ \rightarrow ArNHOH + H_2O \quad (3)$$

To further investigate the electrochemical behavior as a function of pH, the measured CV peak potential, E_p, was plotted between pH 1.98 and 10.0 (Fig. 1D). The plot trends indicated that the peak potential, c, shifted to more negative values with increasing pH (1.98 to 6.10) and the slope for the E_p–pH plot was 53.3 mV/pH. The slope of such plots may be expressed in terms of the number of protons, a, and the number of electrons, n, i.e. slope = $60a/n$ (Sreedhar et al., 2010). In this work the value of $a/n = 0.89 \approx 1$ was obtained. This behavior was consistent with reaction (1) above in which the number of protons equaled the number of electrons. The pH versus E_p plot for peak c1 (Fig. 1D) indicated that the potential remained almost the same as a function of pH in the basic pH region. This observation was consistent with reaction (2) above, in which no protons were involved. The slope of a similar pH versus E_p plot for peak c2 (Fig. 1D) was 70.5 mV/pH, and the value a/n was then evaluated as 1.17/1 or approximately $\approx 4/3$. This experimental result was almost the same as that for reaction (3) above, i.e., the ratio of proton to electron was 4:3. These observations indicate that nitro-radicals could be generated during the reduction of NFZ at relatively high pH, i.e. peak c1 would be associated with a one-electron reduction, and peak c2 would correspond to a three electron/four proton reaction. Thus, for this work, in order to monitor the generation and reduction of nitro-radical anions, solutions of pH 9.10 were selected.

3.1.2. Effect of CV scan rate on absorption

It is important to ascertain if any NFZ is absorbed on the electrode during CV experiments, especially where the electrode is subjected to repeat scans. The peak current (I_{pc}) for NFZ was linear with the square root of the scan rate ($v^{1/2}$) (Fig. 2A). This is consistent with a system under diffusion-control (Arvand et al., 2011). As the scan rate increased from 20 to 320 mV s^{-1}, E_{pa1} and E_{pc1} remained almost constant (Fig. 2B), and this indicated that peaks a1 and c1 were reversible redox peak couples. A plot of E_{pc2} versus ln (v) produced a linear equation: $E_{pc2} = -0.043$ ln (v)–0.598 ($r = 0.997$). The slope of this line may be represented by the equation $-(RT)/\alpha nF$ (Polyanin, 2002), and if the electron transfer number (Section 3.1.1., three electrons were involved in reaction (3), so here $n = 3$) was substituted into this formula, then

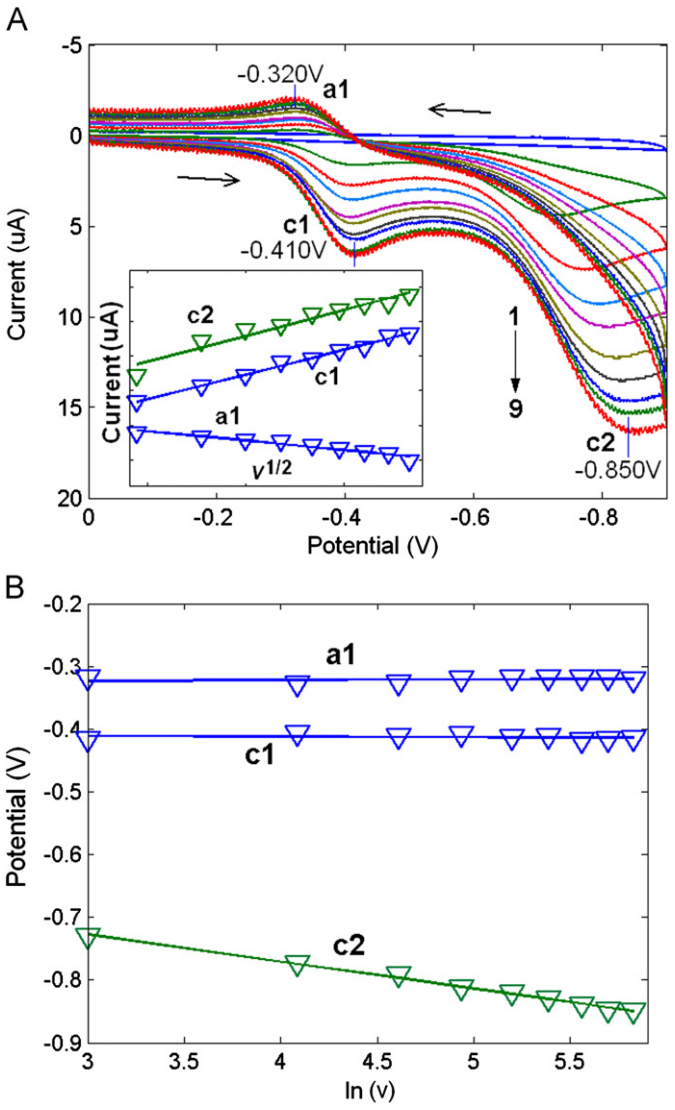

Fig. 2. (A) Cyclic voltammograms of NFZ (2.0×10^{-4} mol L^{-1}) at a GCE with different scan rates (20–320 mV s^{-1}; steps of 40 mV s^{-1}) in Britton–Robinson buffer (pH 9.10). Inset plot: peak current versus square root of scan rate; (B) peak potential versus log (scan rate) plot.

an estimate of the electron coefficient (α) would be 0.20. This indicated that peak c2 was related to an irreversible reduction (generally $\alpha < 0.5$ for an irreversible system (Bard and Faulkner, 2001)).

Thus, it was demonstrated that the two NFZ reduction peaks (peaks c1 and c2) involved the generation and further reduction of nitro-radicals in a protic medium at pH 9.10. The above observations of the effect of the scan rate on the NFZ redox chemistry indicated that the two demonstrated reduction systems were diffusion-controlled. Hence, both NFZ and the nitro-radicals could not be absorbed on the electrode. This conclusion and the preceding results provided a clear pathway for further investigations of the interaction between nitro-radicals and DNA.

3.2. Nitrofurazone interaction with DNA in solution

Interaction between NFZ and DNA was further investigated with the use of the DPV technique (Experiment 2, Section 2.4.). The voltammograms, in the presence of increasing DNA concentration, indicated that the c2 NFZ peak shifted towards negative

potentials (from −0.616 to −0.652 V; Fig. 3); this was consistent with the model when NFZ was bound to DNA mainly by electrostatic interactions (Rauf et al., 2005). The decreasing peak current (peak c2) was proportional to the DNA concentration, which reflected the formation of the DNA–NFZ adducts, and such complexes have been postulated to be electrochemically inactive (Wang et al., 2011). Also, it is interesting to note that only the c2 peak was affected as described above in the presence of DNA; since this peak was associated with the formation of a nitro-radical then the above observations suggested that the interaction of this radical with DNA played an important role in the NFZ–DNA reaction process.

3.3. Characterization of the dsDNA/GCE and the NFZ on the DNA treated micas

The dsDNA/GCE biosensor was investigated with the use of the $[Fe(CN)_6]^{3-/4-}$ complex as an electroactive probe (Section 2.3.). The CV scan of the untreated GCE immersed in a solution of

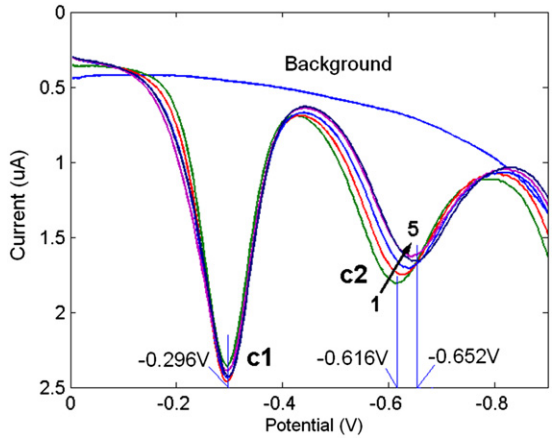

Fig. 3. DPV voltammograms of NFZ (2.0×10^{-4} mol L^{-1}) in the presence of DNA: c_{DNA}=0, 0.005, 0.010, 0.015, and 0.020 mg mL^{-1} at pH 9.10 in a protic medium (curves 1–5).

5.0 mmol L^{-1} $[Fe(CN)_6]^{3-/4-}$ in 0.10 mol L^{-1} KCl displayed a pair of well-shaped redox peaks, which could be ascribed to $[Fe(CN)_6]^{3-}/[Fe(CN)_6]^{4-}$ redox couple. However, when the experiment was repeated with the dsDNA/GCE, the negatively charged DNA on the surface of the GCE electrostatically repelled the negatively charged $[Fe(CN)_6]^{3-/4-}$ in solution. Hence, the $[Fe(CN)_6]^{3-/4-}$ could not bind or intercalate into dsDNA, and consequently, no redox reaction could take place involving the $[Fe(CN)_6]^{3-/4-}$ at the dsDNA/GCE electrode. Thus, as expected, virtually no CV signal of $[Fe(CN)_6]^{3-/4-}$ was observed; the peak current of the $[Fe(CN)_6]^{3-/4-}$ decreased by as much as 99% as compared to curve a, and this implied that the GCE was compactly covered by the dsDNA.

The influence of NFZ on thick or thin DNA mica sheets was investigated by AFM. From Fig. 4A, it was found that the thicker film prepared by evaporation from 1.0 mg mL^{-1} dsDNA could almost completely cover the mica sheet. The formed thin dsDNA layers appear as network structures on the mica sheet at low DNA concentration (Fig. 4C). Diculescu et al. (2005) reported that due to the existence of pores in the DNA structure, misleading results could arise when using a DNA electrochemical biosensor with pores for detection of the DNA–drug interaction. Thus, the prepared electrode with 1.0 mg mL^{-1} DNA (Section 2.3.) is a much more suitable alternative to use in our work. The influence of NFZ on thick or thin DNA deposits on mica sheets was also investigated by AFM. A comparison of Fig. 4A with Fig. 4B, suggests that the fleecy-like structure of dsDNA on mica sheet became tightly packed; however, the DNA network structure changed remarkably after being broken on addition of NFZ (see Fig. 4C and D). Also, after the addition of NFZ, the height of the thick/thin films decreased by 4–5 nm. All of these observations supported our proposition that NFZ can react with dsDNA and break its structure.

3.4. Damage to DNA involving NFZ and the generated short-lived radicals

3.4.1. Indirect detection of DNA damage induced by NFZ

The dsDNA/GCE biosensor was used to investigate any DNA damage that might have been induced by NFZ; the reaction

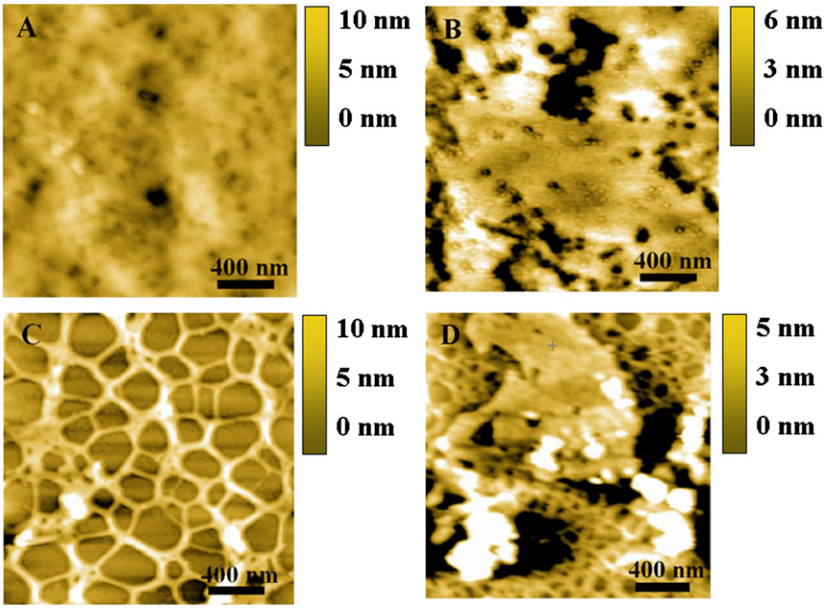

Fig. 4. AFM images of: (A) 30 μL 1.0 mg mL^{-1} dsDNA film; (B) mixed solution: 30 μL 1.0 mg mL^{-1} dsDNA and 5×10^{-3} mol L^{-1} NFZ after evaporation on a mica sheet; (C) 30 μL 10 μg mL^{-1} dsDNA film; (D) diluted mixture of 30 μL 10 μg mL^{-1} dsDNA and 5×10^{-5} mol L^{-1} NFZ after evaporation on a mica sheet.

process was monitored with the use of the $Co(phen)_3^{2+}$ probe, which provided an *in vitro* model to mimic the pathway of DNA damage (Experiment 3, Section 2.4.). The DNA damage in the presence of the complex occurred via the strong intercalative binding of $Co(phen)_3^{2+}$ to the double helix of the DNA (Zhang et al., 2010a). The DPV voltammogram of $Co(phen)_3^{2+}$ at an untreated GCE (curve c; Fig. 5A) was much lower than that when the complex was reacted at the surface of a dsDNA/GCE (curve a); clearly, this peak was much more intense presumably because $Co(phen)_3^{2+}$ can be absorbed on the dsDNA/GCE electrode via intercalation on the adsorbed DNA. This electrode was then treated for 10 min in the NFZ solution, and the corresponding current response of $Co(phen)_3^{2+}$ at dsDNA/GCE significantly decreased (curve b). $Co(phen)_3^{2+}$ is a large metal-chelate, which can strongly combine with DNA and that is why it is sometimes used as to probe indirectly any DNA damage (Zhang et al., 2010a); there is almost no $Co(phen)_3^{2+}$ on the surface of the dsDNA/GCE electrode to be replaced by NFZ. Therefore, the competitive adsorption effect of NFZ is not a major factor for decrease in current. Consequently, in this experiment, the electrode was immersed in the NFZ solution for 10 min without any reduction; thus, nitro-radicals were not generated to damage DNA, and decrease the absorption capacity. Thus, the above argument indicates that when the double helix structure of DNA is damaged by NFZ, the intercalation capacity of $Co(phen)_3^{2+}$ on the electrode is reduced significantly, and a decrease in peak current is observed; also, this argument indicates why the NFZ molecule can be considered as a carcinogen (Takahashi et al., 2000; Bartel et al., 2009).

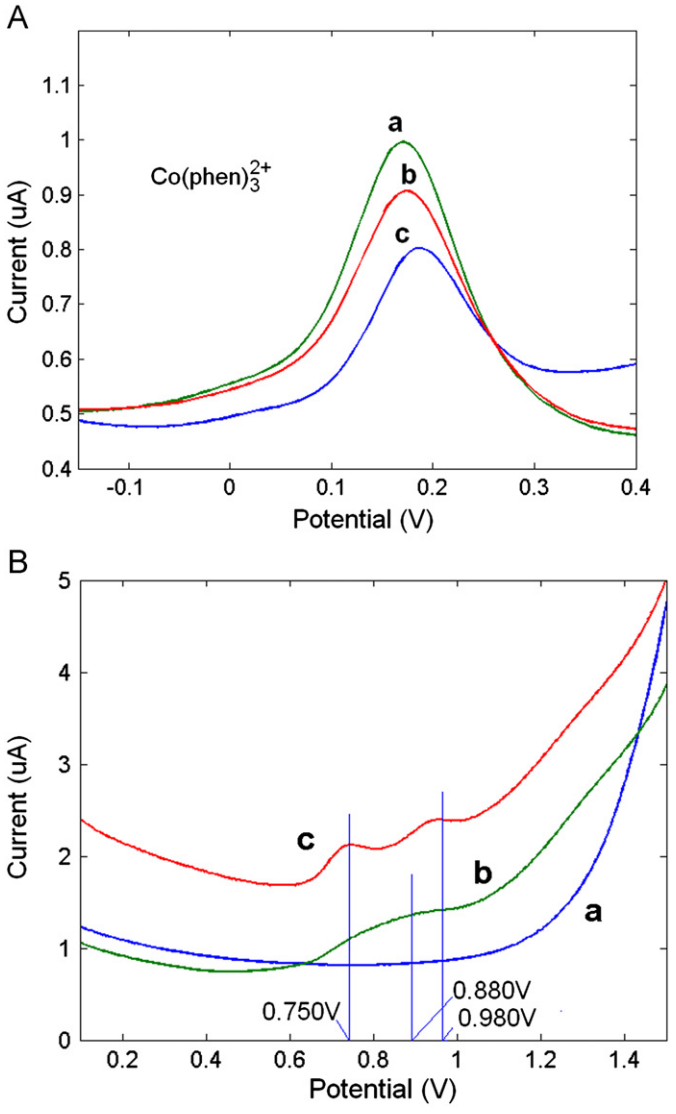

Fig. 5. (A) DPV voltammograms of 5.0×10^{-5} mol L^{-1} $Co(phen)_3^{2+}$ in 10 mM phosphate buffer pH 7.00 obtained at the DNA modified electrode: (a) before, and (b) after the electrode was treated in the NFZ solution for 10 min; (c) untreated GCE. (B) DPV voltammograms using the DNA biosensor in protic medium at pH 9.10: (a) blank, (b) in 2×10^{-4} mol L^{-1} NFZ solution after a 2 min treatment, and (c) after 10 CV scans from 0 to −0.9 V.

3.4.2. *Direct detection of DNA damage induced by nitro-radical anion*

DNA damage induced by nitro-radicals, which are produced by electrochemically reduced NFZ, was investigated at variously treated dsDNA/GCE (Experiment 4, Section 2.4.) with the use of CV. A DPV analysis was performed with each treated dsDNA/GCE biosensor (Fig. 5B). In the absence of NFZ, i.e. in a blank solution (curve a), no oxidation signal of DNA was observed; this is expected if the available DNA bases are protected by the double-stranded DNA. However, if the DNA was damaged then the bases would be exposed and they could be detected electrochemically. In this context, firstly, a small change was noted in the DP voltammogram after the dsDNA/GCE was treated in the NFZ solution; a small broad peak appeared (curve b), which indicated damaged DNA. Then, under the same experimental conditions, the NFZ was reduced over several successive cathodic cycles, from 0 to −0.9 V (10 scans; Vyskočil et al., 2010), and an increase of guanine (750 mV) and adenine (980 mV) peaks was observed (curve c). As previously described (Section 3.1.1.), when NFZ was reduced, nitro-radical anions were formed; hence, the guanine and adenine peaks clearly indicated that the DNA must have been damaged by the reactive nitro-radicals, which resulted in a distortion of the double helix and the consequent exposure of the bases to oxidation. Also, a comparison of the signal intensities from these bases shows that the nitro-radicals exhibit stronger cytotoxicity than the effects of NFZ. Hence, the metabolism of NFZ *in vivo* can bring about more serious carcinogenic effects.

3.5. *Quantitative determination of NFZ and application*

A DPV calibration was obtained with the DNA biosensor for the voltammetric analysis of NFZ in real samples (Section 2.5.). The linear calibration model was: $I = 1.94c_{NFZ} - 1.32$ ($R^2 = 0.9997$), the concentration range and limits of detection were 2.50×10^{-6}–3.75×10^{-5} mol L^{-1} and 8.0×10^{-7} mol L^{-1}, respectively, and nasal drops were analyzed for NFZ (Section 2.5.); the result was 1.2 ± 0.1 mg mL^{-1}.

4. Conclusions

The reduction of NFZ was monitored by CV in protic media at high pH. During this reaction nitro-radicals were generated, and it was demonstrated that the dsDNA damage induced by NFZ and nitro-radicals could be rapidly measured with the use of electrochemical methods. The $Co(phen)_3^{2+}$, a complex and electroactive molecule, provided indirect information for an *in vitro* model to mimic the pathway of DNA damage facilitated by NFZ; this DNA damage, induced by the nitro-radical anions, was investigated by the direct DPV method using a successive cathodic cycling method at the dsDNA/GCE; the results suggested that the nitro-radicals were more cytotoxic than the NFZ molecules. These observations were strongly supported by novel AFM results, which indicated that the tightly packed fleecy-like structure of dsDNA on mica sheets changed remarkably after being broken on

addition of NFZ. Also, the DNA biosensor can be used satisfactorily for analysis of selected pharmaceuticals. Finally, the electrochemical studies with NFZ at the dsDNA/GCE suggest that these techniques would be suitable for in vitro toxicity screening of new chemicals and nanomaterials.

Acknowledgments

The authors gratefully acknowledge the financial support of this study by the National Natural Science Foundation of China (NSFC-21065007), and the State Key Laboratory of Food Science and Technology of Nanchang University (SKLF-MB-201002 and SKLF-TS-200919).

References

Abreu, F.C., Goulart, M.O.F., Oliveira Brett, A.M., 2002. Biosensors and Bioelectronics 17, 913–919.
Arvand, M., Ansari, R., Heydari, L., 2011. Materials Science and Engineering C 31, 1819–1825.
Bard, A.J., Faulkner, L.R., 2001. Electrochemical Methods: Fundamentals and Applications, second ed. Wiley, New York, p. 236.
Bartel, L.C., Montalto de Mecca, M., Castro, J.A., 2009. Food and Chemical Toxicology 47, 140–144.
Bollo, S., Núñez-Vergara, L.J., Martinez, C., Chauviere, G., Périé, J., Squella, J.A., 2005. Electroanalysis 15, 19–25.
Carbajo, J., Bollo, S., Núñez-Vergara, L.J., Navarrete, P., Squella, J.A., 2000. Journal of Electroanalytical Chemistry 494, 69–76.
Chen, L.X., Niu, C.G., Xie, Z.M., Tan, N.Y., 2010. Journal of Analytical Chemistry 65, 260–266.
da S. Julião, M.S., Ferreira, E.I., Ferreira, N.G., Serrano, S.H.P., 2006. Electrochimica Acta 51, 5080–5086.
de Bengoa Vallejo, R.B., Iglesias, M.E.L., Cervera, L.A., Fernandez, D.S., Prieto, J.P., 2011. Journal of the American Academy of Dermatology 64, 328–335.
Diculescu, V.C., Paquim, A.M.C., Brett, A.M.O., 2005. Sensor 5, 377–393.
Escobosa, M.C.M., Quesada, M.C.M., Granados, S.C., Lopez, J.A., 2009. Journal of Investigational Allergology and Clinical Immunology 19, 510–511.
Fotouhi, L., Faramarzl, S., 2004. Journal of Electroanalytical Chemistry 568, 93–99.
Hiraku, Y., Sekine, A., Nabeshi, H., Midorikawa, K., Murata, M., Kumagai, Y., Kawanishi, S., 2004. Cancer Letters 215, 141–150.
International Agents for Research on Cancer (IARC), 2011. Agents Classified by the IARC Monographs, 1–102. World Health Organization, Lyon.
Ito, K., Kajikawa, S., Nii, A., Doi, K., 2005. Experimental and Toxicologic Pathology 56, 333–339.
Khodari, M., Mansour, H., Mersal, G.A.M., 1999. Journal of Pharmaceutical and Biomedical Analysis 20, 579–586.
Liao, T.L., Wang, Y.F., Zhou, X.B., Zhang, Y., Liu, X.H., Du, J., Li, X.J., Lu, X.Q., 2010. Colloids and Surfaces B 76, 334–339.
Lin, S.Y., Jeng, S.L., 2001. Journal of Food Protection 64, 1231–1234.
Ona, K.R., Courcelle, C.T., Courcelle, J., 2009. Journal of Bacteriology 191, 4959–4965.
Pang, D.W., Zhang, M., Wang, Z.L., Qi, Y.P., Cheng, J.K., Liu, Z.Y., 1996. Journal of Electroanalytical Chemistry 40, 183–188.
Polyanin, A.D., 2002. Handbook of Linear Partial Differential Equations of Engineers and Scientists. Chapman & Hall/CRC Press, Boca Raton.
Rauf, S., Gooding, J.J., Akhtar, K., Ghauri, M.A., Rahman, M., Anwar, M.A., Khalid, A.M., 2005. Journal of Pharmaceutical and Biomedical Analysis 37, 205–217.
Sreedhar, M., Reddy, T.M., Balaji, K., Reddy, S.J., 2010. Analytical Letters 43, 674–686.
Takahashi, M., Iizuka, S., Watanabe, T., Yoshida, M., Ando, J., Wakabayashi, K., Maekawa, A., 2000. Cancer Letters 156, 177–184.
Takegawa, K., Mitsumori, K., Yasuhara, K., Moriyasu, M., Sakamori, M., Onodera, H., Hirose, M., Nomura, T., 2000. Toxicologic Pathology 28, 649–655.
Thongsrisomboon, P., Liawruangrath, B., Liawruangrath, S., Satienperakul, S., 2010. Food Chemistry 123, 834–839.
Tittlemier, S.A., Van de Riet, J., Burns, G., Potter, R., Murphy, C., Rourke, W., Pearce, H., Dufresne, G., 2007. Food Additives and Contaminants 24, 14–20.
Tocher, J.H., 1997. General Pharmacology 28, 485–487.
Trossini, G.H.G., Malvezzi, A., T-do Amaral, A., Rangel-Yagui, C.O., Izidoro, M.A., Cezari, M.H.S., Juliano, L., Chin, C.M., Menezes, C.M.S., Ferreira, E.I, 2010. Journal of Enzyme Inhibition and Medicinal Chemistry 25, 62–67.
Tubino, M., Vila, M.M.D.C., Palumbo, M.N., 2009. Journal of the Brazilian Chemical Society 20, 1901–1907.
Vyskočil, V., Labuda, J., Barek, J., 2010. Analytical and Bioanalytical Chemistry 397, 233–241.
Wang, J.R., Zhang, L.Y., 2006. Journal of Liquid Chromatography and Related Technologies 29, 377–390.
Wang, Y.X., Ni, Y.N., Kokot, S., 2011. Analytical Biochemistry 419, 76–80.
Xiong, L., Batchelor-McAuley, C., Goncalves, L.M., Rodrigues, J.A., Compton, R.G., 2011. Biosensors and Bioelectronics 26, 4198–4203.
Xu, J.H., He, X.D., Jin, L.L., Jiang, L., Zhou, Y.F., Kang, Z.H., Peng, R., Shuit-Tong, L., 2011. Electrochimica Acta 56, 5759–5765.
Zhang, W., Yang, T., Li, W.J., Li, G.C., Jiao, K., 2010a. Biosensors and Bioelectronics 25, 2370–2374.
Zhang, Y.L., Zhang, X., Fei, X.C., Wang, S.L., Gao, H.W., 2010b. Journal of Hazardous Materials 182, 877–885.
Zhou, L., Li, J.Q., Lin, X.F., Al-Rasheid, K.A.S., 2011. Aquatic Toxicology 103, 225–232.